Magnetostratigraphy and environmental magnetism in a Pleistocene sedimentary sequence, Marcos Paz, Argentina

Juan Carlos Bidegain, S. Jurado, M. A. E. Chaparro, M. Gómez Samus, S. Zicarelli & A. V. Parodi

Environmental Earth Sciences

ISSN 1866-6280

Environ Earth Sci
DOI 10.1007/s12665-012-1958-7

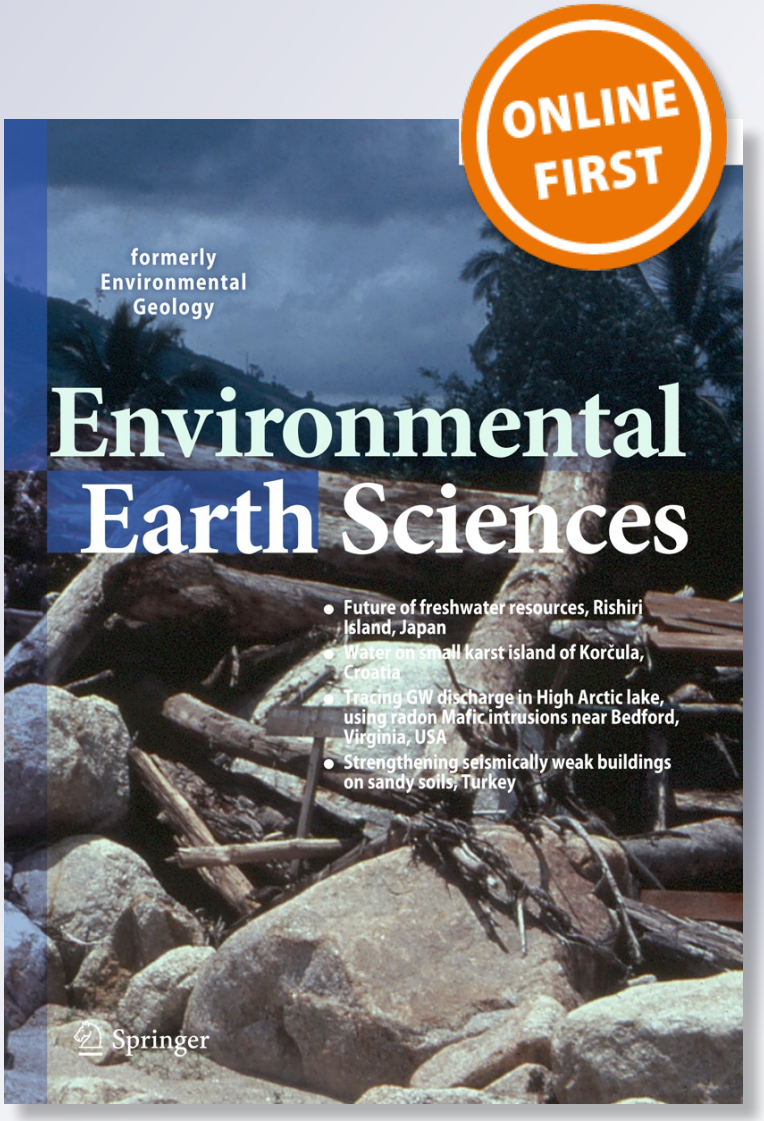

Springer

Environ Earth Sci
DOI 10.1007/s12665-012-1958-7

ORIGINAL ARTICLE

Magnetostratigraphy and environmental magnetism in a Pleistocene sedimentary sequence, Marcos Paz, Argentina

Juan Carlos Bidegain · S. Jurado · M. A. E. Chaparro · M. Gómez Samus · S. Zicarelli · A. V. Parodi

Received: 12 December 2011 / Accepted: 25 August 2012

Abstract Late Cenozoic sediments exposed in a quarry in the locality of Marcos Paz (Buenos Aires province) were studied by applying paleomagnetism and environmental magnetism. The whole sequence, with the exception of the recent soil, belongs to the Pleistocene and is integrated by clayey silts (sandy) and also by a layer of fine sand. Eleven different depositional/postdepositional units, numbered in descending order from unit 1 to 11, were determined. The units 1, 2 and 3 in the upper portion of the geological section should be assigned to Brunhes (<0.78 Ma). Below a depth of 6 m, the reverse polarity zone corresponds to Matuyama (>0.78 Ma). Matuyama magnetozone includes some subzones of normal polarity that should be assigned to the subchron Jaramillo (0.99 Ma) and to the subchron Olduvai (1.9 Ma). The reverse polarity levels determined at the bottom of the profile should be assigned to the lower Matuyama (>1.9 Ma). The highest volume susceptibility values are recorded in the less pedogenized sediments (400×10^{-5}), while the lowest values are always obtained in gleyed horizons (30×10^{-5}). The data support the wind-vigor magnetoclimatological model, although affected by different pedogenesis degrees and weathering as demonstrated by the behavioral pattern of chemical elements.

J. C. Bidegain (✉) · S. Jurado · S. Zicarelli · A. V. Parodi
Laboratorio de Entrenamiento Multidisciplinario para la Investigación Tecnológica (LEMIT), CIC. Calle 52 e/121 y 122, 1900 La Plata, Buenos Aires, Argentina
e-mail: jcbidega@yahoo.com.ar

M. A. E. Chaparro
CONICET-IFAS, Tandil, Argentina

M. Gómez Samus
CONICET-LEMIT, La Plata, Argentina

Keywords Pleistocene · Loess · Magnetostratigraphy · Magnetoclimatology · Paleoenvironments

Introduction

The quarry of Marcos Paz is located on the left bank of a stream, in the headwaters of the Matanza-Riachuelo basin (34°49′20″S. Lat., 58°44′51″W. Long.). Loess (loess-like) sediments with interbedded paleosols exposed on the exploitation fronts of the quarry were studied by means of paleomagnetism and environmental magnetism.

Loess sequences of Argentina are lithologically integrated by sand, silt and clay fractions with predominance of silt (>60 %). The mineralogy is composed of plagioclases, quartz, orthoclase, volcanic glass, altered feldspars, fragments of volcanic rocks and organic opal. The heavy minerals are iron ores (magnetite, ilmenite, limonite), amphiboles and pyroxenes. The silt fraction shows a similar mineralogical composition to the sand fraction; however, the former contains a higher amount of fresh and altered volcanic glass shards. Montomorillonite is the dominant mineral of the clay fraction, although illite, caolinite and chlorite have also been found. According to Teruggi (1957), Argentine loess is "similar in field appearance and texture to the North American and European loess". However, the mineralogical composition is different due to the presence of volcanic-pyroclastic minerals transported by winds to the place of deposition.

Since Heller and Liu (1982) published the first reliable paleomagnetic data from a loess–paleosol sequence in China, several magnetostratigrapahic studies have shown the utility of magnetostratigraphy for relative datation and correlation of loess deposits around the world, as well as locally (Thompson and Oldfield 1986; Maher and Thompson 1991; Orgeira 1987; Bidegain 1991, 1998).

Published online: 11 September 2012

Previously mentioned studies, carried out in Argentina loess deposits, reveal a clear Brunhes/Matuyama zonation as well as the records of sub-zones that have been attributed to Jaramillo and Olduvai subchrons. The aforementioned works, as well as the more recent ones (Bidegain et al. 2009), indicate that the BBM frequently coincides (though not exactly) with a paleosoil showing reverse polarity, first determined in the Hernández quarry (Bidegain 1991) and also by Nabel et al. (1993) who designated the paleosol as geosol Hisisa in the locality of Baradero. The existence of lithological discontinuities among layers and also discordances between the post-Pampean and Pampean sediments, as well as between Ensenada and Buenos Aires Formation, has also been indicated in previous works (Bidegain and Rico 2004). On the other hand, it is important to note studies that establish biozones in the Pleistocene loess (Tonni et al. 1999; Nabel et al. 2000). The authors consider that the Tolypeutes pampaeus Biozone determined in sediments of the Ensenada Formation corresponds to the lower Brunhes and to the upper Matuyama. The *Megatherium americanum* Biozone is recorded exclusively in sediments belonging to the Buenos Aires Formation that show records of normal polarity (Brunhes).

From a magnetoclimatological point of view, several authors have reported their data with high susceptibility values in paleosols and low records in the Chinese loess (Liu et al. 1992; Zhou et al. 1990; Maher and Thompson 1991; Evans and Heller 2003). Also, Béget and Hawkins (1989) reported an inverse relationship between magnetic susceptibility recorded in the par loess–paleosols of Alaska, i.e., loess layers display high susceptibility values, while paleosols display lower ones. Furthermore, Chlachula et al. (1997) reported a similar relationship for Siberian loess. With regard to the Pampean region, it should be pointed out that, originally, winds from west and southwest Argentina carried loess deposits that are observed in several places today. The presence of glass shards, from volcanoes located in central Chile and northern Patagonia, in the loess of the Buenos Aires province, indicates that the west–southwest contribution of wind-carried material has been very important (Teruggi 1957). The rock magnetic data, obtained in loess–paleosol sequences, indicate that the magnetic behavior should be more closely related to the wind-vigor model. Due to that, the less weathered loess shows the highest susceptibility values, at least in several studies carried out in the more humid north of the Buenos Aires Province (Bidegain et al. 2007). The data obtained in paleosols in the same area indicate that the degree of pedogenesis along the Pampean prairie has affected the behavioral model in different ways, which is well within the scope of this contribution. For the present research, previous contributions in other loess sections around the world (Banerjee and Hunt 1993; Maher 1998; Evans and Heller 2003; Maher and Thompson 1991; Banerjee and Hunt 1993; Maher 1998; Chlachula et al. 1997) were also taken into account. Studies applying environmental magnetism indicate that the magnetic signal—as a response of past environmental conditions—should be analyzed carefully as the answer cannot be generalized to all situations. Rather, it is a complex phenomenon which far exceeds the framework of a unique magnetoclimatic model. Moreover, a third model of magnetic behavior has been proposed (Bidegain et al. 2005).

Regional geology

The most important sedimentary units in the northern margin of the Salado Basin have been named Olivos Formation, Paraná Formation, Puelche Formation and Pampean loess, with the aforementioned Ensenada and Buenos Aires formations. The post-Pampean sediments are also loess deposits covering the region and are related to the last glacial event in Patagonia; the recent soil was formed in them. Pleistocene loess is exposed in quarries (as in Marcos Paz quarry) being used as materials for routes. Older sediments must be studied through drillings.

The Olivos Formation was deposited from Eocene to early Miocene, between 45 and 20 million years ago while the Paraná Formation was deposited during the Middle to Late Miocene, between 16 and 5 Ma. The latter formation corresponds to a transgressive/regressive marine event. A warm and shallow sea covered the area leaving oysters at the left banks of the Paraná River during the regressive event. It also left a peneplanation during the regression that has had a strong influence on the subsequent paleo-geomorphology of the Pampean area (Bidegain 1991). Drilling data indicate that Miocene sediments have a thickness of the order of 30–50 m in the subsoil of the city of Buenos Aires. The Puelche Formation (Ituzaingó Formation in Entre Ríos) is mainly integrated by sands (Arenas Puelche), being the most important aquifer in the region. The Puelche Formation lies on the Paraná Formation and is considered to be of Pliocene Age. The so-called "Pampean sediments" lie on the previous fluvial sands; they are loess or loess like with interbedded paleosols, presenting a maximum thickness of about 90 m. The thickness of loess deposits along the continental margin and particularly in the research area is about 40 m.

Methodology

The survey in Marcos Paz began with the field observation of textures and structures, thickness of the layers, types of layers and contact, presence of paleosols, carbonate facies

and paleolagoonal environments, as well as the existence of paleochannels and other structures.

The observation of the different fronts of the quarry made possible the differentiation of 11 stratigraphic layers or units (U1–U11). They are separated by lithologic discontinuities with sharp contacts between them. Some of those units contain well-developed paleosoil horizons; however, other units do not show them. A total of 170 oriented paleomagnetic samples were obtained; 83 of them were selected for the purposes of the present contribution. The distance of sampling varied between 20 and 40 cm, according to the characteristic of the site. The volume susceptibility was measured by an MS2 (Bartington) susceptibility meter with an MS2F sensor. Non-oriented samples were collected to measure the magnetic parameters at the laboratory. Besides, 1/2 kg of representative material was extracted for sedimentological, mineralogical and chemical determinations.

Natural remanent magnetization (NRM) of all samples was measured at the LEMIT laboratory by a magnetometer Minispin (Molspín Ltd). The procedure for determining the ChRM (characteristic remanent magnetization) was performed carefully to avoid the total destruction of remanence, beginning with an AF field as low as 2.5 mT. The maximum field applied was 30 mT in "soft" samples and 70 mT in the "hard" ones, according to the coercivity of remanence. The magnetometer was calibrated with a patron sample (776 mAm^{-1}) every five measurements. Paleomagnetic data were processed by the Super-IAPD program. The data were represented by stereograms, demagnetization curves and Zijderveld "end point" diagrams (Zijderveld 1967) as the directions and intensity in relation to the geological profile.

The volumetric susceptibility (κ), mass-specific susceptibility (χ) and frequency dependence ($\kappa_{FD}\% = 100 \times [\kappa_{470}-\kappa_{4700}]/\kappa_{470}$) were computed. Measurements were carried out using a magnetic susceptibility meter MS2B of dual frequency (470 and 4,700 Hz) produced by Bartington Instruments Ltd. The anhysteretic remanent magnetization (ARM) was imparted superimposing DC fields of 10, 60 and 90 μT to an AF of 100 mT, using a partial ARM (pARM) device attached to a shielded demagnetizer from Molspin Ltd. The remanent magnetization after each step was measured by a Molspin Ltd. Minispin fluxgate spinner magnetometer. Related parameters, such as the anhysteretic susceptibility (κ_{ARM}), King's plot (κ_{ARM} vs. κ, King et al. 1982) and the κ_{ARM}/κ-ratio (Dunlop and Özdemir 1997) were also calculated.

For IRM acquisition studies, each sample was magnetized by exposing it to DC fields from 1.7 to 2,470 mT and using an ASC Scientific model IM-10-30 pulse magnetizer. The remanent magnetization was also measured using the previously mentioned magnetometer.

Owing to these measurements, IRM acquisition curves and saturation of IRM (SIRM) values were obtained. Besides, ARM/SIRM and SIRM/χ ratios were determined using forward DC fields. Remanent coercivity (H_{CR}) and S-ratio (=$-$IRM$_{-300}$/SIRM, with IRM$_{-300}$ the acquired IRM at a backfield of 300 mT) were calculated from IRM measurements using backfield once the SIRM was reached. Additional measurements using a new experimental method were carried out in order to discriminate magnetic phases. This method was developed due to the responses of different assemblages of magnetic materials when subjected to a pulse magnetizing field and a demagnetizing AF. Essentially, this method separates the bulk backfield IRM curve into two individual magnetic phases experimentally. For details and discussion about the method, the reader is directed to Chaparro and Sinito (2004).

The chemical analysis of elements was performed by X-ray fluorescence using an X-ray spectrometer model SPECTRO IQ II. The procedure with the samples began with the drying and careful mixing of the sediments. As a secondary step, a binder BM-0002-1 (FLUXANA) was added to avoid the movement of the grains when handling the material and performing the measurements. The added binder was in the relation 5:1 by weight. Then, pills of 32 mm in diameter and 3 and 5 mm in thickness were prepared with the help of a press, using a pressure of 15 tons.

Analysis of results

Geology

Figure 1 shows the sequence of loess/paleosols in the Marcos Paz quarry; the photograph provides an idea about the place of sampling. The geological profile on the right of the figure shows the layers (units 1, 2, etc.) determined and sampled in the section of 18 m. Some layers did not show the same thickness as in the photo because they were sampled where they had better exposure. For instance, layer U2 is thicker on the right of the site as shown in the photograph (Fig. 1).

The main portion of the sequence corresponds to the Ensenada Formation, while the Buenos Aires and post-Pampean sediments are very poorly represented. With the exception of unit 1, all the units are disposed concordantly and the contacts among units are sharp contacts that generally coincide with the top of a Bt or a calcrete horizon.

The recent soil was developed in loess (La Postrera) deposits, mainly silty loam, that were attributed to the last glacial stage and was labeled as U1; the parent loess was dated by OLS to 19 Ka (Bidegain et al. 2011). The U1 lies in discordance on well-developed paleosols (pedocompex)

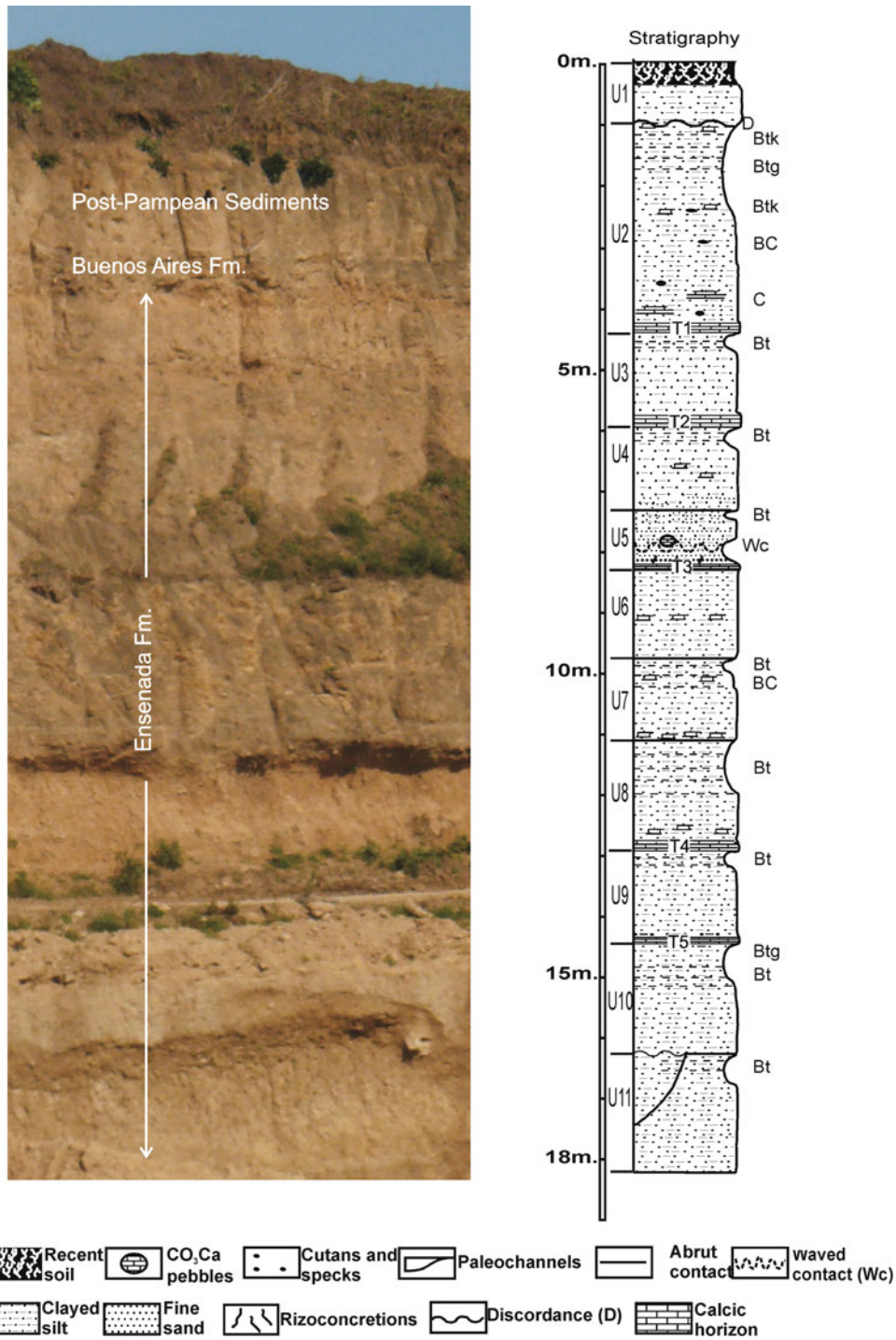

Fig. 1 The geological section is integrated by the Ensenada Formation, Buenos Aires Formation and post-Pampean sediments. Eleven units (U1–U11), integrated by loess (loess-like) and paleosols were determined

composed of Btk, Btg, Btk and C horizons grouped in the U2 that presents a calcrete horizon at the base (T1). The boundary U2/U3 should correspond to the limit between Buenos Aires and Ensenada formations that might be related to one discordance, as was suggested in other localities (Bidegain and Rico 2004). However, the presence of the calcrete horizon (T1) inhibits the differentiation of such discordance here. The unit labeled U3 is composed of silty loam with one silty clay paleosol on the top. A new calcrete horizon at the base of this unit is also represented (T2).

The U4 is integrated by silty loam to loam sediments ending with a Bt horizon that is laterally replaced by a gley horizon. The U5 is composed of sandy loam at the top and fine sands, without cementation, at the base. A very hard layer, cemented by calcium carbonate (T3), showing

rhizoconcretions, is represented at the bottom of the unit. The U6 is composed of silty loam to loam with carbonate concretions of different shape and size, particularly at the middle of this unit. The U7 is silty loam having finer grain size than the previous U6 and a Bt horizon on the top. The BC and Ck horizons at the base of this unit indicate the influence of pedogenesis downward. U8 is mainly composed of silty loam to silt and shows a conspicuous and well-structured Bt horizon with coarse prisms in the upper part and a calcareous horizon (T4) at the base. Unit U9 is composed of silty loam and is massive and compact, presenting also a Bt horizon at the top that is clayey and structured in prisms with calcareous concretions. A calcrete horizon is also represented at the base (T5). The U10 is a silty loam sediment with a Bt horizon on the top; onlying the paleosoil is a gleyed horizon (Btg). The U11 shows coarse grain size than the previous unit; it is silty loam to loam with a paleosol at the top. Conspicuous paleochannel containing clay pebbles of different sizes and iron concretions (pisolitas) of some 5 mm in diameter are also represented at this level.

Paleomagnetism

The short thickness of Argentine loess, in relation to other loess regions of the world (particularly China), undoubtedly affect not only the number of magnetic changes (Brunhes, Matuyama Jaramillo, Olduvai, Jaramillo, etc.), but also the magnitude of each of these events. Due to the lack of sedimentary information, normal and reverse records of magnetic polarity in the Argentine loess are frequently condensed. The declination (D) and inclination (I) as the intensity of NRM, in relation to the geological units, are indicated in Fig. 2. On the right of the same figure, the magnetostratigraphy (according to Cande and Kent 1995) has been indicated.

The units labeled U1, U2 and U3, down to the calcareous level indicated as T2 correspond to the Brunhes normal polarity (<0.78 Ma) magnetozone. The BBM (boundary Brunhes/Matuyama), is related to the Bt horizon in the boundary U3/U4. The layers U4, U5, U6 and U7 present levels of reverse polarity and are assigned to upper Matuyama. Sandy levels (U5) do not have any kind of compaction and provide anomalous directions. Such behavior can be attributed to the unique characteristics of the material, which create an intrinsic impossibility in providing reliable data. The controversial directions obtained in unit 5 have been interpreted taking into account the stratigraphy. Overlying U4, as well as the underlying units U6 and U7, presents reverse polarity directions; therefore, U5 is interpreted as belonging to Matuyama (older than 0.78 Ma). The unit U8 is represented by a conspicuous pedocomplex with a well-marked Bt horizon showing a clear concave molding at the top. The base of U8, which is a less pedogenized horizon (BC), also presents normal polarity directions that are assigned to Jaramillo (0.99–1.05 Ma). Reverse anomalous polarity directions are recorded below the U8, which seems to be related to the existence of a conspicuous gap. These levels seem to indicate a condensed record of some reverse polarity zones; because of that, they were assigned to middle Matuyama (1.05–1.78 Ma). A great portion of U9 and the upper part of U10 present samples with normal polarity directions and were assigned to Olduvai (1.78–2.02 Ma). Reverse polarity directions obtained at the base of the profile were assigned to lower Matuyama.

The existence of differences in the concentration of magnetic minerals along the profile is evident due to the range of variation in the intensity of the NRM. The lower ($I°$) values were between 2 and 4 mA/m, while the highest were between 50 and 70 mA/m. Due to these differences, the magnetic behavior of samples was also different when demagnetizing.

Figure 3 shows some of the typical magnetic behavior of paleomagnetic samples of Marcos Paz, demagnetized by AF. The results are represented through the use of stereographic projections, demagnetization curves and Zijderveld diagrams. The sample labeled MPF3 (a) with $I° = 28.7$ mA/m corresponds to lower Matuyama. The magnetic directions seem to correspond to a normal polarity sample in the first steps of treatment. The inclination is affected at 7.5 mT peak field, but the declination remains as a normal polarity sample, even overcoming the mean field demagnetization at 10 mT. Approaching a higher AF demagnetization field (about 20 mT), both reverse polarity directions are consistent. In the "end point" diagram for this sample, the straight fall toward the origin occurs from early stages of "cleaning", suggesting that magnetite is the main carrier of remanence (specifically, titanomagnetites), probably with some contribution of secondary magnetization (maghemite?). A secondary oxidation seems to have been acting, but it is impossible to record any antiferromagnetic phase through this method.

Figure 3b shows the normal polarity directions of a sample with a stable behavior of demagnetization when applying AF. The initial intensity (NRM) of the sample is 23.873 mA/m and it was necessary to apply a field of 70 mT to overcome the 10 % of the $I°$ ($I = 0.151$ mA/m). The threshold of 10 % seems to be a suitable limit to be considered due to the stability of remanence at 60 mT of applied field ($I = 2{,}134$ mA/m).

The directions of magnetization are stable and the intensity of remanence falls straight forward to the origin in the "end point" diagram, corresponding to the "soft" behavior of samples. The antiferromagnetic contribution seems to be rejected in this case.

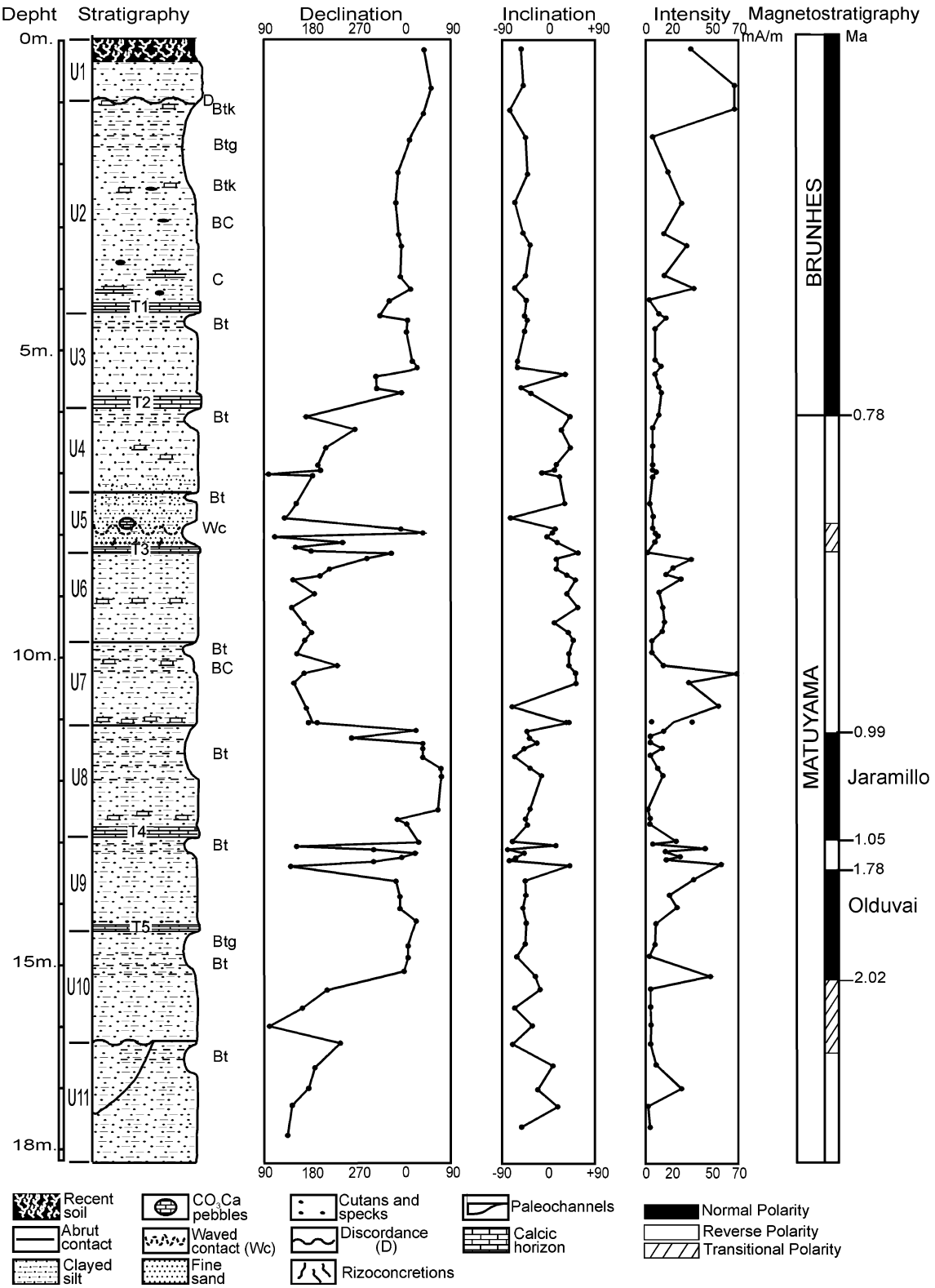

Fig. 2 The paleomagnetic directions and the intensity of remanence (NRM) in relation to the geological profile. The magnetostratigraphy established is shown on the right of the figure

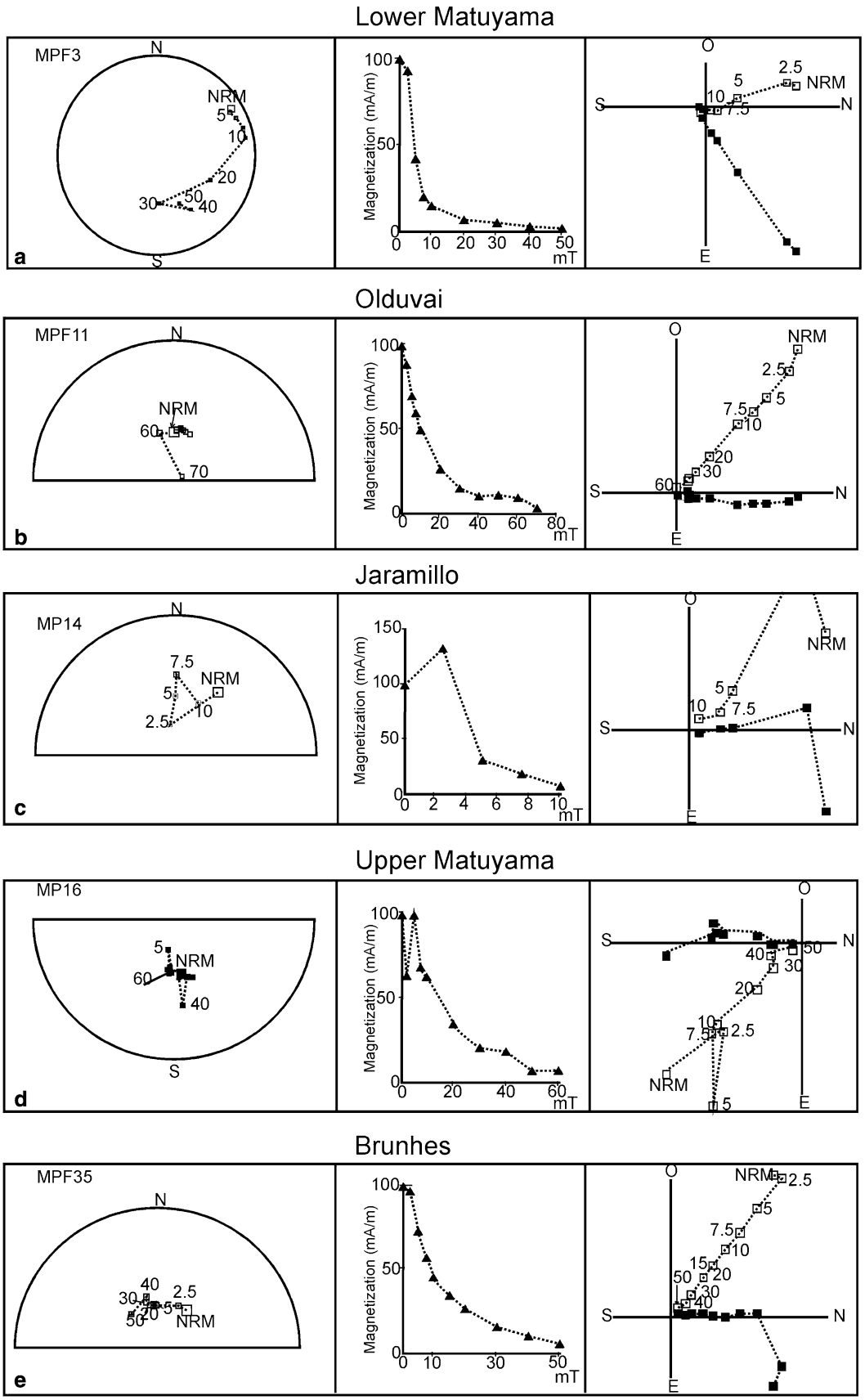

Fig. 3 Stereographic projection, demagnetization curves and Zijderveld diagrams corresponding to some of the samples analyzed

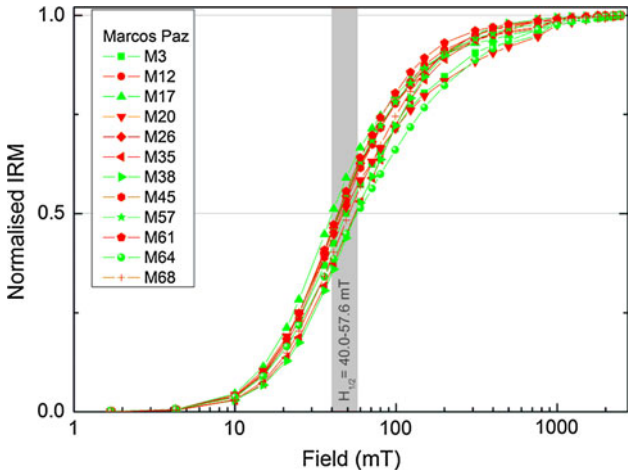

Fig. 4 IRM acquisition curves of the samples of Marcos Paz

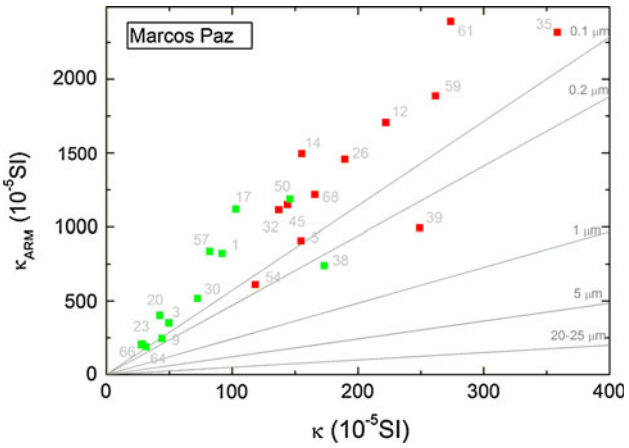

Fig. 6 Values of κ_{ARM} versus the values of κ corresponding to the samples of Marcos Paz, displayed in the King's plot

The sample MP14 (c) in the sector assigned to Jaramillo has a lower intensity value than samples MPF3 and MPF11 (13.558 mA/m). However, the lowest values are around 2 mA/m in the most weathered horizons. A viscous component of magnetization is removed at field as low as 2.5 mT. A change in the direction of both vertical and horizontal components in the Zijderveld diagram indicates that the decay through the end point should correspond to magnetite. The directions remain stable up to 10 mT of peak field applied, as indicated in the stereoplot. The magnetization is very soft because the intensity falls below 1 mA/m at 15 mT of applied field. The increase of intensity at 2.5 mT peak field, indicated by the demagnetization curve, might have been produced by secondary oxidation. The sample MP16 (d) corresponds to upper Matuyama, with an initial intensity (I°) of 58.4 mA/m, which is considerably higher than in the previous sample. This sample shows viscose components of magnetizations that are eliminated at low fields (below 5 mT). From 7.5 mT applied field, the intensity falls abruptly, the MDF overcomes at 20 mT and the intensity at 50 mT peak field is below the initial intensity (Int = 3.7 mA/m). All the directions are in the southern hemisphere from the first steps of the treatment.

Samples of the sector assigned to Brunhes (e) show very stable directions that do not experience any considerable change during the treatment as indicated in Fig. 3e.

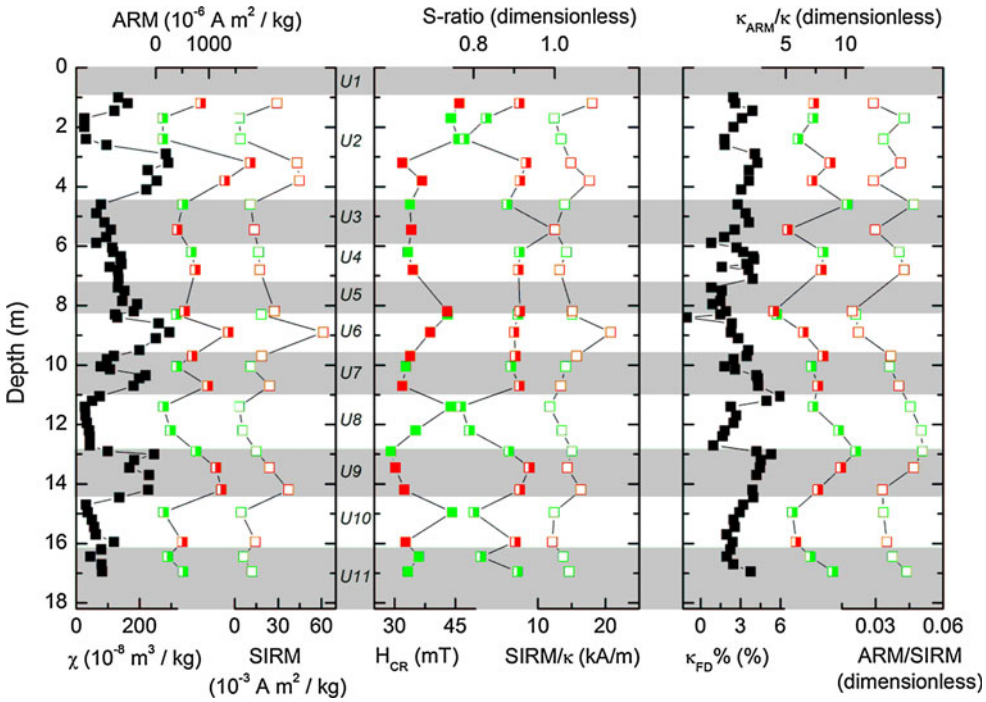

Fig. 5 The concentration-dependent (χ, ARM and SIRM) parameters as the H_{CR}, S-ratio, SIRM/κ and grain size-dependent parameters in relation to the sequence studied

The directions at I° (19,226 mA/m) are in the northern hemisphere, $D = 34.4$ and $I = -49.3$. At 50 mT of applied field, the intensity decreases down to 1.189 mA/m and the directions do not change considerably; $D = 328$ and $I = -53$. As for the other samples, the chosen values for the representation in Fig. 2 correspond to the AF at 40 mT ($D = 349.8$, $I = -45.5$); the intensity is around 10 % of the initial one (I°).

The existence of discontinuities—in continental sediments—affects the accuracy of the sedimentation rate estimation. However, Nabel and Valencio (1981) consider that such discontinuities are irrelevant, studying a 10 m sequence of loess/paleosols in the Buenos Aires City. With the help of paleomagnetic reversals, the authors estimate that the lower and medium portions (7 m) of the profile have a sedimentation rate of 20 mm/1,000 years, while the top of the studied sequence (3 m) has 7 mm/1,000 years.

Using the criterion of continuity applied by the previously mentioned authors, some similarities appear, but also dissimilarities owing to the considered periods appear in Marcos Paz. Considering the Brunhes Normal Chronozone (0–0.78 Ma), the sedimentation rate in the locality studied should be 7.14 mm/1,000 year, and the reverse Matuyama (between 1.8 and 0.78 Ma) should be 7.35 mm/1,000. However considering Jaramillo alone, the sedimentation rate should be 28 mm/1,000 years and for Olduvai 9 mm/1,000 years.

Environmental magnetism

The variation of humid/dry climate that caused the sequence of loess/paleosols in the studied quarry indicates the cyclic variation during the last (at least) 2.6 Ma, creating a characteristic model of magnetic behavior. Such model (Bidegain et al. 2005) of magnetic behavior is characterized by higher susceptibility values in the parent material and lower susceptibility values in paleosols. The region under study is temperate-humid with 16.9° of annual average temperature and 1,100 mm/year rainfall presently.

A set of samples was collected for measurement of magnetic parameters at the selected sites. This was performed taking into account the existence of loess (loess-like) sediments and interbedded paleosols. Each sample was packed in a plastic bag in the field. In the laboratory,

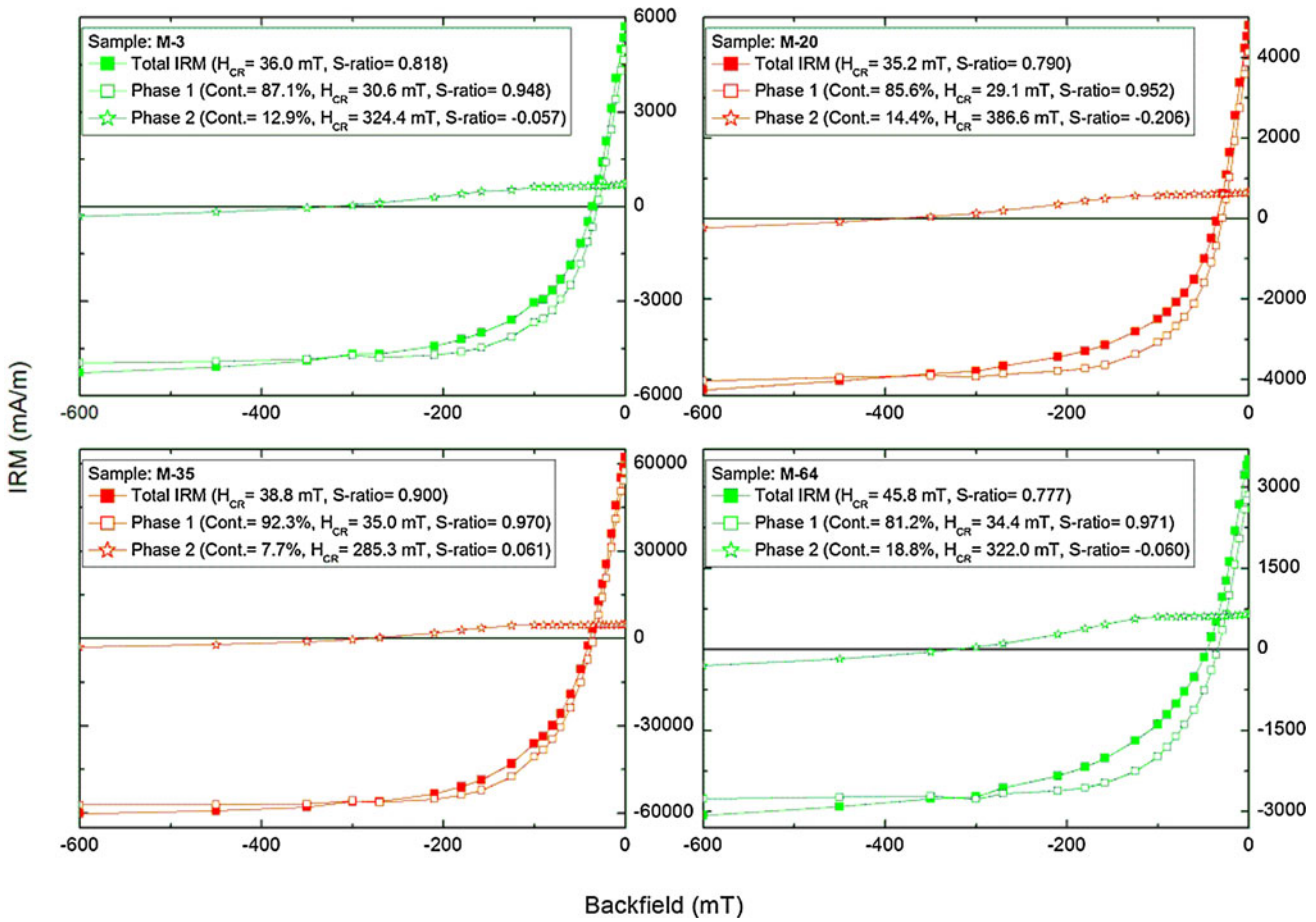

Fig. 7 The contribution of subordinate magnetic phases (antiferromagnetic) in the obtained IRM

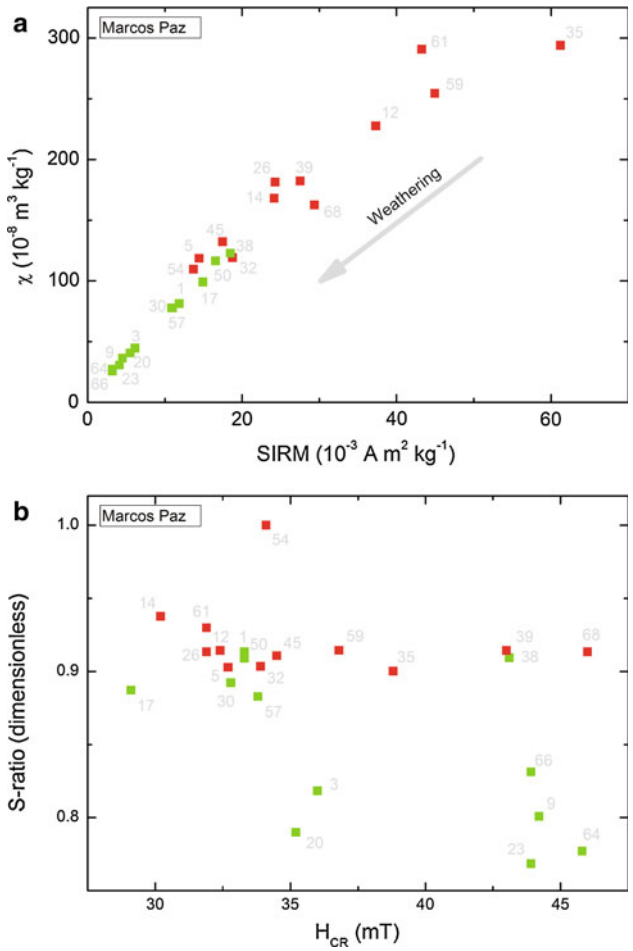

Fig. 8 **a** Values of χ versus SIRM indicating the trend of weathering. The values corresponding to the less affected parent materials are shown in *red* and the most weathered materials in *green*. The mixing zone corresponds to transition zones among the units in the profile. **b** The S-ratios versus the coercivity of remanence

after drying and sieving, two subsamples were obtained; one of them was kept in a plastic container ($\sim$11.5 cm^3) and fixed using a solution of sodium silicate for magnetic measurements, while the other one was preserved in a small bag for other determinations. The IRM acquisition measurements show the dominance of ferrimagnetic minerals with curves that reach their 95 % saturation at 300 mT. As seen in Fig. 4, some of the selected samples (e.g., M3, M20 and M64) demonstrated an additional (harder) magnetic phase.

Magnetic concentration (χ, ARM and SIRM), feature (H_{CR}, S-ratio and SIRM/κ) and grain size (κ_{FD} %, κ_{ARM}/κ-ratio and ARM/SIRM)-dependent parameters are indicated in Fig. 5.

The concentration-related parameters display similar variations along the profile. As observed, the maximum values are up to one order of magnitude higher than the minimum values. The main profile variations correspond to changes in concentration of magnetic minerals that are identified as magnetic enhancement. The changes in magnetic mineralogy and grain size recorded in the first part of the profile (Unit 1–6) and in Unit 11 are in agreement with the concentration trend. For example, concentration highs coincide with lows in H_{CR} and highs in κ_{ARM}/κ-ratio (ARM/SIRM), and vice versa; hence, changes in concentration are accompanied by the input of softer magnetic minerals as well as by the presence of finer magnetic grains.

The values of κ_{ARM} and κ for all samples are displayed in the King's plot (Fig. 6). It is possible to observe in a great portion of the analyzed samples that the magnetic grains fall below 0.1 μm. Another interesting application is to consider these data with reference to the parental material (in red) and palepedological horizons (in green). The mixing of data between 100 and 200 κ (10^{-5} SI) only reflects either BC horizons or loess-like layers, but neither pristine loess nor Bt horizons.

Magnetic parameters, especially H_{CR}, and their analyses, suggest that the magnetic signal of the samples of Marcos Paz is mainly controlled by a magnetite-like phase. The values of H_{CR} vary between 29 and 46 mT; lower values are in agreement with the characteristic values of magnetite (Peters and Dekkers 2003). Higher values can correspond to titanomagnetite and/or the presence of harder magnetic minerals. Applying voltametry and other non-magnetic techniques; in similar sediments Rico et al. (2009), indicate that besides hematite, maghemite also seems to be present. The presence of hematite can be determined from separation methods of IRM acquisition and backfield (Chaparro and Sinito 2004; Chaparro et al. 2005). According to the authors, the presence of subordinate magnetic phases was detected for some selected samples: M3, M35, M20 and M64 (Fig. 7). These phases have contributions to the total IRM (backfield) between 7.7 and 18.8 % with H_{CR} values of 285.3–386.6 mT, which are indicative of hematite minerals. Figure 8a indicates the trend of weathering (see arrow) by using the ratio χ versus SIRM. Paleosols data are represented in green, while loess and loess-like sediments are represented in red. The lowest susceptibility and SIRM values correspond to the most weathered levels (gley). The mixing zone in the diagrams (red and green values) also corresponds to a transition zone among horizons: between loess U4 and the paleosoil on the top, between loess U6 and paleosoil of U7, between loess U6 and the caliche T3.

Figure 8b represents the S-ratios versus the coercivity of remanence of loess and paleosols samples. The range of variation in Hcr is similar for both (loess/paleosols). However the threshold 0.9 of S-ratio seems to be an approximated boundary between loess (red) and paleosol (green) S-ratios, where the lowest values always correspond to gleyed horizons.

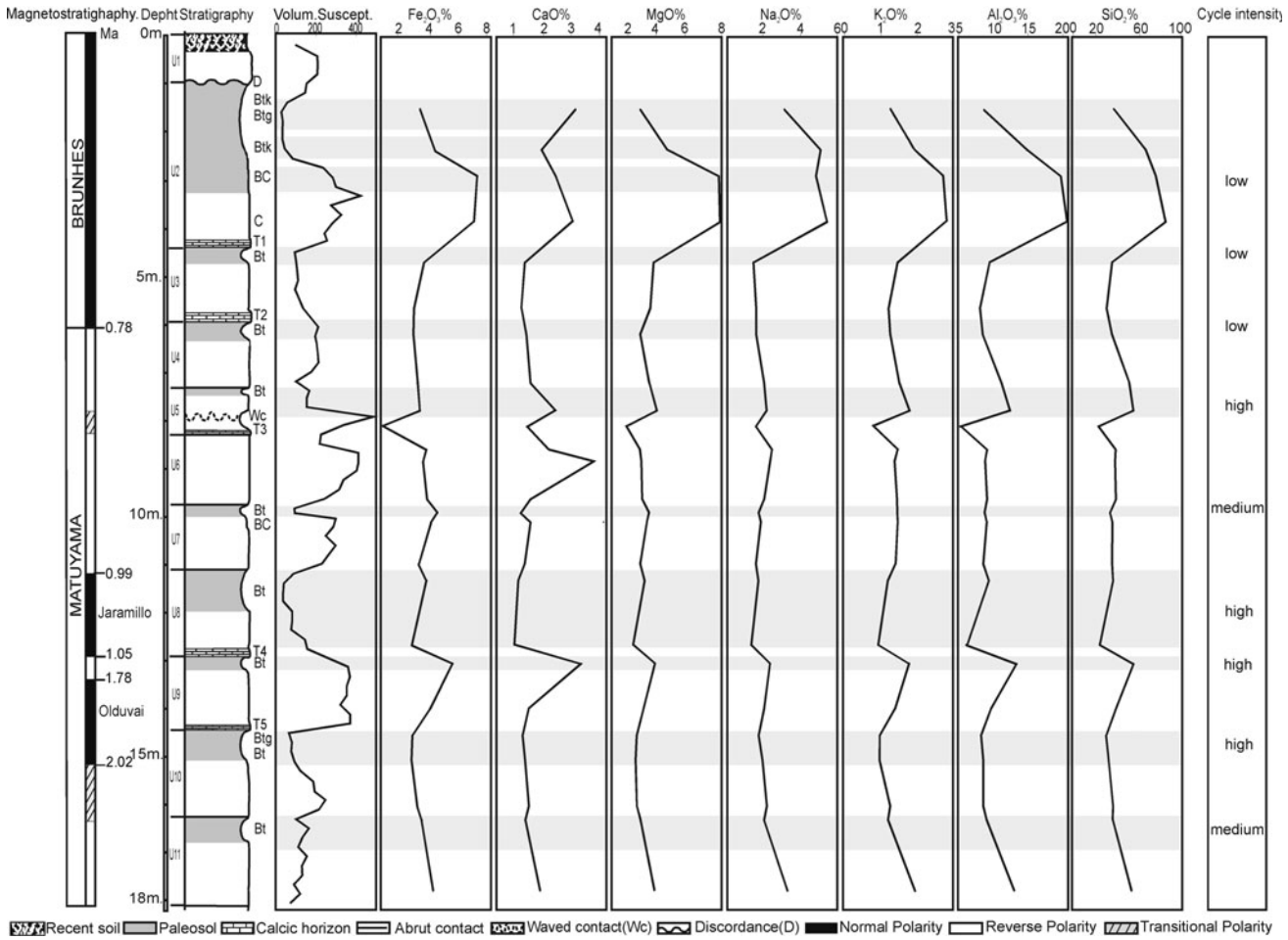

Fig. 9 The Brunhes/Matuyama zonation, the paleopedologic profile, the volumetric susceptibility and the concentrations of chemical elements

Chemical analysis

Figure 9 indicates the obtained magnetostratigraphy, the paleopedologic profile, the volumetric susceptibility and the concentrations of elements expressed in percent. The concentration of the elements seems to have been strongly affected by weathering along the profile. The chemical index of alteration is calculated from the quantitative analysis of chemical composition and is based on the relationships between mobile and immobile oxides.

$$\text{CIA} = \text{AL}_2\text{O}_3/(\text{AL}_2\text{O}_3 + \text{CaO} + \text{Na}_2\text{O} + \text{K}_2\text{O}) \text{ x } 100.$$

According to Aristizábal et al. (2009), the variation in the CIA index depends on the variation in humidity degree.

The analysis of chemical parameters reveals that according to the so-called "CIA index", the values of loess layers differ from those obtained in pedogenized and weathering materials. As first approach, it was estimated that if the variation between loess and paleosols was low (1–2), the weathering was also low. The highest differences in the CIA index (>4) correspond to the most intensely weathered horizons. Consequently, intermediate weathering conditions correspond to those values of CIA index between 2 and 4. Figure 10a shows the location of samples studied. To establish the weathering patterns, a triangle A–CN–K (Fig. 10b) was used. The end A corresponds to 100 % of Al_2O_3, CN represents the sum of Ca and Na oxides and K corresponds to 100 % of K_2O. For the purposes of better visualization of the results, the lower end of the triangle represents 40 %. Therefore, the value of each sample varies from 40 to 100 %, where 100 % of A corresponds to the most intensively weathered materials. They are those materials associated with kaolinite–gibbsite clays.

The line of feldspar has a value of 50 % with plagioclase at one end and potassium feldspar in the other. According to the authors mentioned above, the line of 75 % corresponds to clays as a derivate product of weathering of feldspar (smectite and illite).

The patterns of weathering of the different loess and paleosoil samples follow a straight line toward the end (Al_2O_3) as indicated by the arrow. This trend seems to be independent

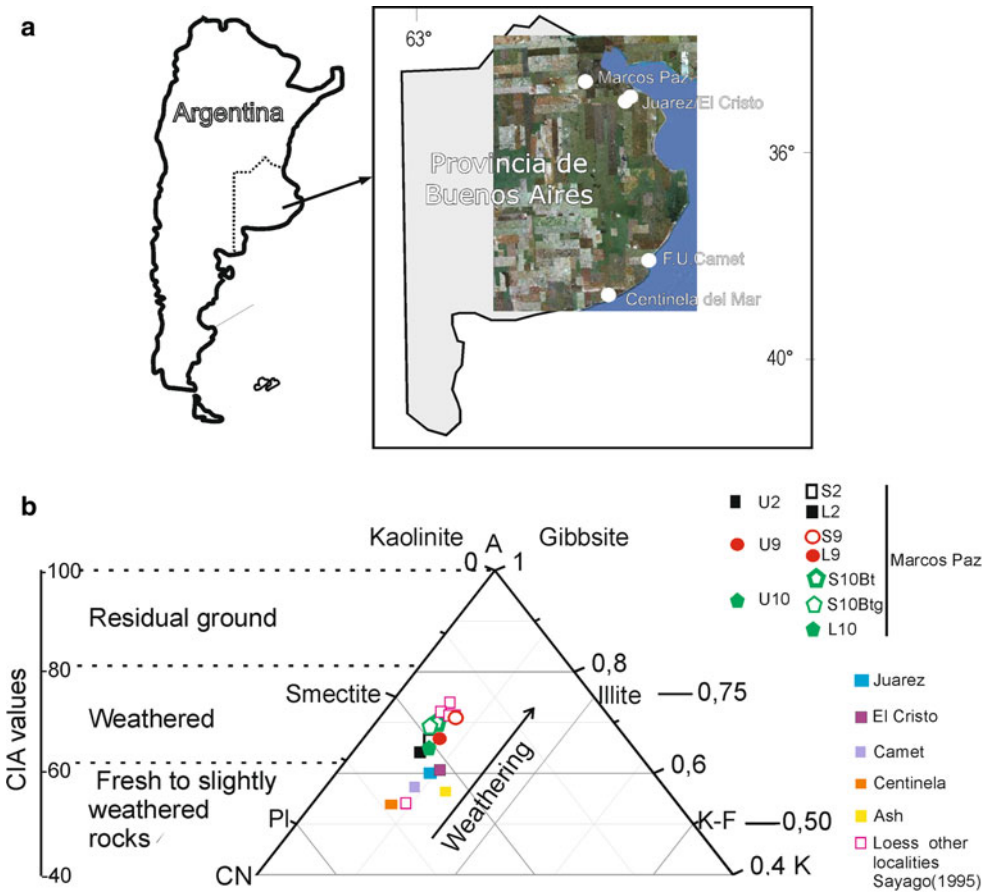

Fig. 10 **a** Map indicating the location of samples studied. **b** Diagram of A–CN–K representing the weathering index (CIA) obtained in loess and paleosols of the Pampean region. The *arrow* indicates the trend of weathering

of the intensity and duration of the physical and chemical processes involved in the loess/paleosoil analyzed.

According to the geological field observation where chemical and environmental parameters were applied, it can be stated that all the studied units have been affected by weathering. However, by using the triangle to represent the CIA values, it is observed that no samples fall at the end of A or even close to this end, which would indicate an extreme situation.

The degradation of feldspar and the formation of clay minerals are the dominant processes during the chemical weathering of loess in the Pampean region. This process occurs in such a way that Ca, Na and K are generally removed from the feldspars, increasing the proportion of Al in the weathering products (Nesbitt and Young 1982). Besides the concentration of SiO_2, the concentration of Al_2O_3 is considerably greater than the concentration of the other elements as indicated in Fig. 9. In the triangle (Fig. 10), the linear displacement toward the A end would, in a projection, cut the A–K side once the plagioclase has been removed. This, however, was not observed. Therefore, the samples are richer in plagioclase than in potassium feldspars. Loess (loess-like) samples of Marcos Paz (L2, L9 and L10) are located in the triangle very close to the composition of the smectites (that would derivate from the weathering of the plagioclases) and are placed far from the illite and kaolinite. Such positioning of the loess-like materials in the triangle should indicate that all the layers of the quarry have been affected by hydromorphism. Moreover, all the samples placed between 60 and 70 of CIA values in the triangle would indicate clays caused by weathering. According to Fedo et al. (1995), fresh minerals and rocks, regardless of their composition, will record similar CIA value (around 40–50), while completely weathered materials will have CIA values around 100.

The samples labeled S2, S9, S10Bt and S10Btg correspond to the most weathered horizons and originated from loess materials. The sediments of the late Cenozoic in the Pampean region, as stated in the present work, have been affected more or less by the weathering process. However, in some localities, it is possible to determine the presence of loess less affected by these processes and also without noticeable signs of pedogenesis. To establish the behavior of the latter, less pedogenized materials have also been incorporated into the triangle.

One sample from the Juárez quarry (34°57′0″S, 57°53′00″W) and the other from El Cristo quarry (34°55′S, 57°57′W; La Plata locality), have been included in the

triangle (Fig. 10b). The CIA values for both samples are very similar (around 60). Furthermore, a sample of loess from Mar del Plata (Camet; 37°53′34.3″S, 57°31′16″W) and another of volcanic ash from the El Chaitén eruption (42°54′26.1″S, 71°18′31.8″W), which occurred in 2008 (fresh material), also provide very similar CIA values (58 and 57, respectively). A loess sample from Centinela del Mar (38°26.3′4″S, 58°13′25.4″W), showing the lowest CIA values (54), has also been indicated. The latter should correspond to the lowest reached degree of weathering, according to this method. Besides, the chemical analysis of loess samples from Tucumán to Miramar, reported by Sayago (1995), was also plotted in the A–CN–K triangle. Almost all of the Sayago data may be considered as weathered loess; however, the chemical composition of the Miramar sample reported by Sayago (1995) corresponds to less weathered loess, giving a low CIA value, as it is with the previous mentioned Centinela sample (Fig. 10b). Miramar is a locality near Centinela, which is indicated in the map (Fig. 10a).

Discussion

The magnetostratigraphic zonation obtained in Marcos Paz has a precedent in the Hernández quarry in La Plata, where two levels of normal polarity were identified within the Matuyama polarity zone. Besides, five complete paleomagnetic profiles carried out in the Gorina quarry of La Plata showed normal polarity levels, which were assigned to Jaramillo, at the bottom of the quarry (Bidegain 1998). More recently, Heil et al. (2010), in the same quarry of Gorina, found normal polarities within Matuyama that they assigned to Jaramillo and Olduvai. However, a controversy has arisen, in recent years, with regard to the relationship between paleomagnetic boundary and geological boundary. Erroneously, Heil et al. (2010), maintain the relationship between the BBM and the lithostratigraphic units locally designated as Formation Buenos Aires and Formation Ensenada. However, it should be pointed out that this interpretation has been specifically corrected in more recent works, which clarify the concept as follows: the boundary between the lithostratigraphic units Buenos Aires and Ensenada formations has no connection with the Brunhes–Matuyama boundary. Moreover, the BBM has been defined, in several contributions, within the Ensenada Formation (Bidegain and Rico 2004; Bidegain et al. 2005, 2007, 2009).

The limitations imposed by the discontinuities in the depositional process determine the magnetic record. It is evident, however, judging by the contributions of several researchers that one and, in some cases, two normal polarity subzones may be obtained in the Matuyama chronozone of the Pampean loess.

Variation of the chemical elements determined by Rx fluorescence has been related to the variation of environments along the profile. Several variations of parameters related to the environmental changes, however, can be appreciated along the profile. The variation of the chemical elements and susceptibility values indicate five environmental cycles during Brunhes. Welded paleosols in U2 should probably be assigned to more than one cycle. An increase of chemical parameters to the base of the U2 indicates the presence of less weathered levels.

The upper Matuyama is represented by six cycles of relative climatic variation (wet/dry). Except for the levels of U6, there does not seem to be noticeable changes in concentration of elements in this part of the profile. The Jaramillo subchron presents a drop in susceptibility values as well as in the concentrations of major elements. This relation should indicate a dominant wet climatic condition. In addition to the susceptibility values, the concentration of chemical elements show high and low values in the very short record assigned to middle Matuyama.

Olduvai seems to be represented by a dry cycle in the upper part and by a humid cycle in the lower part. Drier climate conditions are associated with a glacial period and humid condition with the interglacial period. Susceptibility and chemical parameters follow the same trend, although moderately.

Three different environmental conditions should be represented at the base of the sequence by loess-like deposits, paleosols and reworked clayey silts (U10 and U11). Below the paleosol assigned to lower Olduvai, there is a layer of loess-like sediments (U10), where the susceptibility values increase, although chemical data hardly follow the same trend. The difference between both susceptibility and chemical parameters is more difficult to appreciate in U11 due to the pedogenesis that occurred on reworked alluvial sediments.

Conclusions

The units of the upper section of the profile of Marcos Paz (U1, U2, U3) correspond to the Brunhes normal polarity chronozone (<0.78 Ma). From 6 m deep and down to the base of exploitation (Unit 11), the paleomagnetic records refer to the Matuyama reverse chronozone (>0.78 Ma). The normal polarity records within Matuyama have been referred to Jaramillo (0.99 Ma) and Olduvai (1.9 Ma), both normal subchrons of polarity. In addition, at the base of the quarry, U10 and U11 units have levels of reverse polarity that would correspond to lower Matuyama (>1.9 Ma).

The behavior of magnetic susceptibility is consistent with the model of behavior determined in the north of the Buenos Aires Province. Higher susceptibility values

correspond to the less pedogenized parental materials (around 400 $\times$ 10^{-5} SI) and the lowest values correspond to the more intensely weathered horizons (20–40 $\times$ 10^{-5} SI). Mass susceptibility and the other concentration-related parameters follow the pattern of volume susceptibility measured in the field. The highest SIRM values were obtained in less pedogenized materials, while the lowest SIRM values always corresponded to more intensely weathered horizons. The H_{CR} values are generally between 35.2 mTt and 45.8 mT, thus indicating the ferromagnetic contribution.

Antiferromagnetic contribution, however, has been estimated between 7.75 and 18.8 %, producing an increase in the coercivity values in some particular levels (weathered levels). Interparamagnetic relations appear to be suitable to indicate the different weathering degrees along the loess sequences. The relationship between Karm and K (King plot) not only indicates that the magnetic signal is represented by magnetic particles below 0.1 μm, but also that the lower values of both parameters refer to the highest weathered layers. The mass susceptibility versus SIRM values are also appropriate for indicating the differences in weathering degrees among layers. Such differences occur in such a way that Ca, Na and K are generally removed from the feldspars, increasing the proportion of Al in the weathering products. The index of weathering employed (CIA) indicates that all the samples are placed between 60 and 70 of the CIA values. The data indicate also that clay minerals were mainly produced by weathering. Loess and loess-like sediments less affected by pedogenesis and weathering showed the lowest values of CIA (54).

Acknowledgments This work was carried out with the financial support of the LEMIT and Scientific Research Commission of the Buenos Aires Province. The authors are grateful to Dr. Marcelo Toledo for having indicated the quarry of Marcos Paz as an appropriate locality for study. The authors would like to thank the CONICET and UNCPBA as well as Mr. Paul Zubeldia (IFAS-UNICEN) for his technical support and Christian Vassillón for providing the volcanic ash.

References

Aristizábal E, Roser B, Yokota S (2009) Patrones e índices de meteorización química de los depósitos de vertiente y rocas fuentes en el Valle de Aburrá. Bol Ciencias de la tierra 25:27–42

Banerjee SK, Hunt C (1993) Separation of local signals from the regional paleomonsoon record of the Chinese loess plateau: a rock-magnetic approach. Geophys Res Lett 20:843–846

Béget JE, Hawkins DB (1989) Influence of orbital parameters on Pleistocene loess deposition in central Alaska. Nature 337:151–153

Bidegain JC (1991) Sedimentary development, magnetostratigraphy and sequence of events of the late Cenozoic in Entre Ríos and surrounding areas in Argentina. PhD Thesis. University, Stockholm, Sweden, 128 p

Bidegain JC (1998) New evidence of the Brunhes–Matuyama polarity boundary in the Hernandez-Gorina Quarries, north-west of the city of La Plata, Buenos Aires. Quat South Am Antarct Peninsula 11:207–229

Bidegain JC, Rico Y (2004) Mineralogía magnética y registros de susceptibilidad en sedimentos cuaternarios de polaridad normal (Brunhes) y reversa (Matuyama) de la cantera de Juárez, provincia de Buenos Aires. Revista de la Asociación Geológica Argent 59:451–461

Bidegain JC, Evans ME, van Velzen AJ (2005) A magnetoclimatological investigation of Pampean loess. Geophys J Int 160: 55–62

Bidegain JC, van Velzen AJ, Rico Y (2007) The Brunhes/Matuyama boundary and magnetic parameters related to climatic changes in quaternary sediments of Argentina. J S Am Earth Sci 23:17–29

Bidegain JC, Rico Y, Bartel A, Chaparro MAE, Jurado SS (2009) Magnetic parameters reflecting pedogenesis in Pleistocene Loess deposits of Argentina. Quat Int 209:175–186

Bidegain JC, Jurado SS, Gómez Samus ML (2011) Magnetoestratigrafía en una secuencia de loess/paleosuelos del Pleistoceno en Marcos Paz, Provincia de Buenos Aires. Argentina. Revista de la Asociación Geológica Argen 68(4):606–614

Cande SC, Kent DV (1995) Revised calibration of the geomagnetic polarity timescale for the Late Cretaceous and Cenozoic. J Geophys Res 100:6093–6095

Chaparro MAE, Sinito AM (2004) An alternative experimental method to discriminate magnetic phases using IRM acquisition curves and magnetic demagnetisation by alternating field. Rev Bras Geof 22(1):17–32

Chaparro MAE, Lirio JM, Nuñez H, Gogorza CSG, Sinito AM (2005) Preliminary magnetic studies of lagoon and stream sediments from Chascomus Area (Argentina)—magnetic parameters as indicators of heavy metal pollution and some results of using an experimental method to separate magnetic phases. Environ Geol 49:30–43

Chlachula J, Rutter NW, Evans ME (1997) A late Quaternary loess–paleosol record at Kurtak, southern Siberia. Can J Earth Sci 34: 679–686

Dunlop J, Özdemir Ö (1997) Rock magnetism: fundamentals and frontiers. Cambridge University Press, Cambridge, p 573

Evans ME, Heller F (2003) Environmental magnetism: principles and applications of enviromagnetics. Academic Press, Elsevier Science, Amsterdam, p 299

Fedo CM, Nesbitt HW, Young GM (1995) Unraveling the effects of potassium metasomatism in sedimentary rocks and paleosols, with implications for paleoweathering conditions and provenance. Geology 23:921–924

Heil CW Jr, King JW, Zárate MA, Schultz PH (2010) Climatic interpretation of a 1.9 Ma environmental magnetic record of loess deposition and soil formation in the central eastern Pampas of Buenos Aires, Argentina. Quat Sci Rev 30:1–14

Heller F, Liu TS (1982) Magnetostratigraphical dating of loess deposits in China. Nature 300:431–433

King J, Banerjee SK, Marvin J, Özdemir Ö (1982) A comparison of different magnetic methods for determining the relative grain size of magnetite in natural materials: some results from lake sediments. Earth Planet Sci Lett 59:404–419

Liu XM, Shaw J, Liu TS, Heller F, Naoyin Y (1992) Magnetic mineralogy of Chinese loess, and its significance. Geophys J Int 108:301–308

Maher AB (1998) Magnetic properties of modern soils and quaternary loessic paleosols: paleoclimatic implications. Palaeogeogr Palaeoclimatol Paeleoecol 137:25–54

Maher AB, Thompson R (1991) Mineral magnetic record of the Chinese loess and paleosols. Geology 19:3–6

Nabel PE, Valencio DA (1981) La magentoestratigrafía del ensenadense de la ciudad de Buenos Aires: su significado geológico. Revista de la Asociación Geológica Argent XXXVI 1:7–18

Nabel P, Camilion MC, Machado GA, Spiegelman AT, Mormeneo L (1993) Magneto y litoestratigrafía de los sedimentos pampeanos en los alrededores de la cuidad de Baradero, Pcia. de Buenos Aires. Revista de la Asociación Geológica Argent 48:193–206

Nabel PE, Cione A, Tonni EP (2000) Environmental changes in the Pampean area of Argentina at the Matuyama–Brunhes (C1r–C1n) Chrons boundary. Paleogeogr Paleoclimatol Paleoecol 162:403–412

Nesbitt HW, Young GM (1982) Early Proterozoic climates and plate motions inferred from major element chemistry of lutites. Nature 199:715–717

Orgeira MJ (1987) Estudio paleomagnético de sedimentos del cenozoico tardío en la costa atlántica bonaerense. Revista de la Asociación Geológica Argent 42:362–376

Peters C, Dekkers MJ (2003) Selected room temperature magnetic parameters as a function of mineralogy, concentration and grain size. Phys Chem Earth 28:659–667

Rico Y, Bidegain JC, Elsner CI (2009) Synthetic and natural iron oxide characterization through microparticle voltammetry. Geofísica Internacional 48(2):221–236

Sayago JM (1995) The Argentine neotropical loess: an overview. Quat Sci Rev 14:755–766

Teruggi ME (1957) The nature and origin of Argentine loess. J Sediment Petrol 27:322–332

Thompson R, Oldfield F (1986) Environmental magnetism. Allen and Unwin, London, p 227

Tonni EP, Nabel P, Cione AL, Etchichury M, Tófalo R, Scillato Yané G, San Cristóbal J, Carlini A, Vargas D (1999) The Ensenada and Buenos Aires formations (Pleistocene) in a quarry near La Plata, Argentina. J South Am Sci 12:273–291

Zhou LP, Oldfield F, Wintle AG, Robinson SG, Wang JT (1990) Partly pedogenic origin of magnetic variations in Chinese loess. Nature 346:737–739

Zijderveld JDA (1967) A.C. demagnetization of rocks: analysis of results. In: Collinson DW, Creer KM, Runcorn SK (eds) Methods in paleomagnetism. Elsevier, Amsterdam, pp 254–286